ANTIOXIDANTS & REDOX SIGNALING
Volume 6, Number 1, 2004

Original Research Communication

Combined Superoxide Dismutase/Catalase Mimetics Alter Fetal Pulmonary Arterial Smooth Muscle Cell Growth

STEPHEN WEDGWOOD[1] and STEPHEN M. BLACK[1–3]

ABSTRACT

Reactive oxygen species (ROS) are known to play an important role in the proliferation and viability of vascular smooth muscle cells. We have shown previously that treatment of fetal pulmonary arterial smooth muscle cells (FPASMC) with concentrations of 25 μ*M* and higher of EUK-134, a superoxide dismutase/catalase mimetic, decreased cell viability via the induction of apoptosis. Here we demonstrate a dose-dependent decrease in serum-induced FPASMC growth at lower doses of EUK-134. This was due to the attenuation of FPASMC proliferation rather than the induction of apoptosis. Moreover, we found that the inhibition of FPASMC proliferation was observed using EUK-134 at concentrations as low as 5 μ*M*. This inhibition of proliferation correlated with a 31% decrease in superoxide levels, as estimated using the oxidation of dihydroethidium. Flow cytometry revealed an increase in FPASMC in G_2 after 24 h of exposure to 10 μ*M* EUK-134. This was associated with a twofold increase in levels of the cell-cycle regulatory protein p21. This, together with our previous data, suggests that ROS levels determine the rate of FPASMC proliferation and, when below a threshold level, trigger apoptosis. Titration of ROS with antioxidants may help to prevent, or reverse, the vascular remodeling manifest in many cardiovascular disease states. *Antioxid. Redox Signal.* 6, 191–197.

INTRODUCTION

INCREASING EVIDENCE suggests that reactive oxygen species (ROS) such as superoxide anions and hydrogen peroxide can stimulate vascular smooth muscle cell (SMC) growth (16, 23). These ROS appear to be produced by SMC in response to treatment with growth factors known to cause SMC proliferation (9, 23). Recently, we have shown that the vasoactive peptide endothelin-1 stimulated ovine fetal pulmonary arterial SMC (FPASMC) proliferation via an induction of ROS (26). In addition, elevation of ROS levels was mitogenic for these cells (26). In contrast, other experiments have shown that antioxidant treatment (24), or overexpression of catalase (5), reduced viability and induced apoptosis in vascular SMC. Similarly, we have shown that antioxidant treatment or inhibition of the superoxide-producingenzyme NADPH oxidase decreased viability and induced apoptosis in FPASMC (26). Overall, these data suggest that increased levels of ROS stimulate SMC proliferation, whereas decreased ROS levels can prevent proliferation and induce apoptosis. Antioxidants that are able to decrease these ROS may therefore prove to be an effective therapy for diseases arising from excessive vascular muscularization.

Salen-manganese complexes are low-molecular-weight synthetic compounds that possess superoxide dismutase and catalase activities, catalytically removing superoxide and hydrogen peroxide, respectively (3, 8). These compounds are thought to exhibit better stability and bioavailability than proteinaceous antioxidant enzymes. Furthermore, their catalytic mode of action may prove more effective than low-molecular-weight antioxidant compounds. EUK-134 is one such superoxide dismutase/catalase mimetic (2). This compound has been demonstrated to reduce brain infarct size in a rat model of stroke (2), a condition thought to arise due to increased ROS production. In addition, EUK-134 has been shown to be protective in a mouse model of amyotrophic lateral sclerosis (12), in an organ cul-

[1]Department of Pediatrics, Northwestern University Medical School, Chicago, IL 60611-3008.
[2]Department of Biomedical and Pharmaceutical Sciences and [3]International Heart Institute of Montana, University of Montana, Missoula, MT.

ture model for Alzheimer's disease (1), and against kainate-induced neurotoxicity (17).

Recently we demonstrated an induction of apoptosis in FPASMC treated with EUK-134 at concentrations of 25 μ*M* and higher (25). Furthermore, lower doses of EUK-134 attenuated serum-induced FPASMC proliferation without stimulating programmed cell death (25). The purpose of this study was to identify the molecular mechanisms of EUK-134-mediated decreases in FPASMC growth. In doing so, it is hoped that better treatment and prevention strategies for cardiovascular diseases associated with alterations in SMC growth may be developed.

MATERIALS AND METHODS

EUK-134

EUK-134 was generously provided by Dr. Susan Doctrow (Eukarion, Inc., Bedford, MA, U.S.A.). This salen-manganese compound is a modified version of the prototype EUK-8 and exhibits greater catalase activity. Synthesis, structure, and catalytic activities of EUK-134 have been described previously (2).

Cell culture

Primary cultures of FPASMC from sheep were isolated by the explant technique as described previously (26). Identity was confirmed as FPASMC by immunostaining (>99% positive) with antibodies against α-smooth muscle actin, calponin, and caldesmon. This was taken as evidence that cultures were not contaminated with fibroblasts or with endothelial cells. All cultures for subsequent experiments were maintained in Dulbecco's modified Eagle's medium (DMEM) supplemented with 10% fetal calf serum (Hyclone, Logan, UT, U.S.A.), antibiotics, and antimycotics (both from MediaTech, Herndon, VA, U.S.A.) at 37°C in a humidified atmosphere with 5% CO_2/95% air. Cells were utilized between passages 3 and 10.

Cell proliferation assays

FPASMC at ~2,500 cells per well were seeded onto 96-well plates (Costar, Corning, NY, U.S.A.) (~25% confluence) and allowed to adhere for at least 18 h. The initial number of viable cells was then determined to correct for differences in starting cell number between experiments, and to monitor changes in cell number over time. This was determined using the Cell Titer 96 AQ_{ueous} One Solution kit (Promega, Madison, WI, U.S.A.), the basis of which has been shown to be a reliable alternative to [^{3}H]thymidine incorporation (6). The tetrazolium reagent is bioreduced to a colored product, the quantity of which is proportional to the number of metabolically active cells. Twenty microliters of reagent was added directly to cells in 100 μl of medium, and following a 2-h incubation period at 37°C the absorbance at 492 nm was read using a Labsystems Multiskan EX plate reader (Fisher, Pittsburgh, PA, U.S.A.). For the proliferation assay, cells were washed with phosphate-buffered saline (PBS) and incubated with media containing 10% fetal calf serum and 0–10 μ*M* EUK-134. The Cell Titer 96 AQ_{ueous} One assay was repeated as described above to determine the number of viable cells at 24 h after treatment.

Terminal deoxynucleotidyltransferase (TdT) dUTP nick end-labeling (TUNEL) analysis

TUNEL analysis was performed on EUK-134-treated FPASMC using the DeadEnd Colorimetric Apoptosis Detection System (Promega). FPASMC were seeded onto 96-well plates and incubated with 0, 10, or 50 μ*M* EUK-134 as described above. After 30 h, cells were washed in sterile PBS and fixed in 4% (vol/vol) paraformaldehyde for 20 min at 4°C. Cells were washed twice in PBS and then incubated with TdT and reaction mix including fluorescein-12-dUTP for 1 h at 37°C. Cells were washed for 30 min in 2× saline–sodium citrate buffer and then incubated with PBS plus 4′,6-diamidino-2-phenylindole (DAPI; 5 μ*M*) for 15 min at room temperature. DAPI is a blue fluorescent nuclear stain, and this step ensured that approximately equal cells were imaged in each slide. The cells were visualized by fluorescence microscopy as described below, with excitation at 485 nm and emission at 530 nm.

Fluorescence analysis

FPASMC were seeded onto 96-well plates (Costar) and allowed to adhere for at least 18 h. Cells were then washed in PBS and incubated in DMEM containing 0–10 μ*M* EUK-134 for 30 min. Dihydroethidium (DHE, 20 μ*M*; Molecular Probes, Eugene, OR, U.S.A.) or dichlorodihydrofluorescein diacetate (H_2DCF-DA, 20 μ*M*; Molecular Probes) was added to the media 15 min before the end of the experiment. Cells were washed with PBS and imaged using a Nikon Eclipse TE-300 fluorescent microscope. DHE-stained cells were observed after excitation at 518 nm and emission at 605 nm. Fluorescent images were captured using a CoolSnap digital camera and the average fluorescent intensities (to correct for differences in cell number) quantified using Metamorph imaging software (Fryer, Huntley, IL, U.S.A.). Statistical analyses between treatments were carried out as detailed below (see Statistical analysis).

Flow cytometry

FPASMC were seeded onto six-well plates (Costar) at 125,000 cells per well (~25% confluence) and allowed to adhere for 18 h. Cells were washed three times in PBS and incubated in serum-free DMEM for 24 h for cell synchronization. Cells were then incubated in DMEM supplemented with 10% fetal calf serum and 0 or 10 μ*M* EUK-134 for 24 h. Cells were washed in PBS, trypsinized, pelleted, and reconstituted at 1×10^6 cells per milliliter of stain solution: 50 μg/ml propidium iodide (Sigma, St. Louis, MO, U.S.A.), 180 U/ml RNase A (Sigma), 0.1% Triton-X (Fisher), 3.4 m*M* sodium citrate (Sigma), 3% polyethylene glycol (Bufferad Inc., Lake Bluff, IL, U.S.A.). After incubation at 37°C for 20 min, 1 ml of salt solution was added: 50 μg/ml propidium iodide, 0.1% Triton-X, 3.6 *M* sodium chloride (Fisher), 3% polyethylene glycol. Cells were stored overnight in the dark at 4°C. Analysis was performed using a Coulter Epics XL-MCL flow cytometer and data interpreted using Mod-Fit software.

Immunocytochemistry

FPASMC were seeded onto 96-well plates and incubated with 0 or 10 μ*M* EUK-134 as described above. After 24 h,

cells were washed in PBS and fixed in 4% (vol/vol) paraformaldehyde at 4°C for 20 min. Cells were washed three times in PBS for 5 min, then treated with 0.1% IGEPAL CA-630 (Sigma) for 1 min at room temperature. After three PBS washes, cells were blocked in 5% (wt/vol) nonfat dry milk (Nestle, Solon, OH, U.S.A.), 0.05% Tween (Fisher) in PBS for 60 minutes at room temperature. Cells were washed three times in PBS and incubated with primary antibodies against cyclin A (2 μg/ml; Santa Cruz, Biotechnology, Santa Cruz CA, U.S.A.), cyclin D1 (1 μg/ml, Santa Cruz), p21 (6 μg/ml, Oncogene, Boston, MA, U.S.A.), and p27 (2 μg/ml, Oncogene) in 5% bovine serum albumin (Sigma), 0.05% Tween in PBS at 4°C for 16 h. Cells were washed three times in PBS and incubated with goat anti-mouse IgG conjugated to Oregon Green (Molecular Probes) for cyclin A, p21, and p27, and with goat anti-rabbit IgG conjugated to Rhodamine Red (Molecular Probes) for cyclin D1, in 5% nonfat dry milk, 0.05% Tween in PBS for 60 minutes in the dark at room temperature. Cells were washed three times in PBS and visualized using fluorescence microscopy with excitation at 485 nm and emission at 530 nm as described above. Quantification of the fluorescent signal was determined using Metamorph imaging software using our previously published procedures (28).

Statistical analysis

Changes in viable cell number, percentage cell number, and fluorescence intensities in response to EUK-134 treatment were calculated and expressed as means ± SD. Comparisons between treatment groups were made by ANOVA using the GB-STAT software program. A $p < 0.05$ was considered statistically significant.

RESULTS

ROS such as superoxide and hydrogen peroxide are important mediators of vascular SMC growth and viability. We have shown previously that the superoxide dismutase/catalase mimetic EUK-134 induced apoptosis in FPASMC at doses of 25 μ*M* and higher (25). Here we performed cell viability assays on FPASMC treated with media containing 10% serum plus 0–10 μ*M* EUK-134 to determine the effects of lower doses of this compound. After 24 h, 5 and 10 μ*M* EUK-134 significantly attenuated serum-induced proliferation of FPASMC ($P < 0.05$ versus untreated, Fig. 1) without reducing the number of viable cells initially seeded (Fig. 1). This suggests that lower doses of EUK-134 inhibit FPASMC proliferation without inducing programmed cell death.

To confirm this, we performed TUNEL analysis on FPASMC treated with 10 μ*M* EUK-134 for 24 h. The absence of TUNEL-positive nuclei at this concentration (Fig. 2) indicates a decrease in proliferation rather than a reduction in FPASMC number via apoptosis. However, apoptosis was detected by the addition of a control of 50 μ*M* EUK-134 (Fig. 2).

We have previously shown that treatment of FPASMC with EUK-134 resulted in dose-dependent decreases in superoxide and hydrogen peroxide levels, as detected by DHE and H_2DCF-DA fluorescence, respectively (25). Exposure to 5 μ*M* EUK-134, which attenuated serum-induced proliferation, resulted in a 31% decrease in DHE fluorescence and a 71% decrease in H_2DCF-DA fluorescence (25). EUK-134 at 25 μ*M*, which induced apoptosis, reduced DHE fluorescence by a further 50%, but reduced H_2DCF-DA fluorescence by only an additional 7% relative to 5 μ*M* EUK-134 (25). As this range of superoxide concentration was much greater than for hydrogen peroxide, here we exposed FPASMC to lower doses of EUK-134 to correlate the inhibition of FPASMC proliferation with the percentage decrease in superoxide levels. Our results indicate that the lowest concentration of EUK-134 (5 μ*M*) that significantly reduces FPASMC proliferation decreases cellular superoxide levels by 31% ($p < 0.05$ versus untreated; Fig. 3).

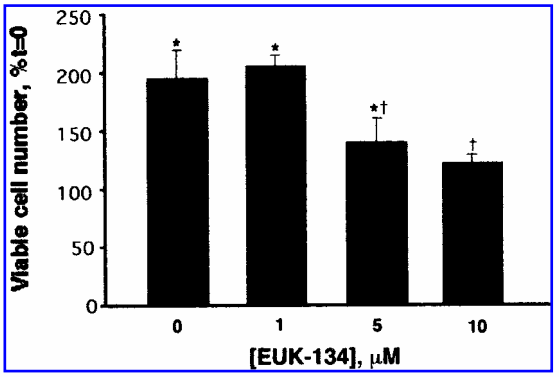

FIG. 1. Serum-induced proliferation of FPASMC in response to EUK-134 treatment. FPASMC at ~2,500 cells per well were seeded onto 96-well plates. The initial cell number at $t = 0$ was determined using the Cell Titer 96 AQ_{ueous} One Solution kit (Promega). Cells were incubated in 10% fetal calf serum and 0–10 μ*M* EUK-134 at 37°C for 24 h, and the Cell Titer 96 AQ_{ueous} One assay was repeated. Values are means ± SD; $n = 8$ samples. *$p < 0.05$ versus initial number of cells at $t = 0$; †$p < 0.05$ versus 0 μ*M* EUK-134.

We next used flow cytometry to identify the mechanisms of EUK-134-mediated attenuation of FPASMC growth. After 24 h, 10 μ*M* EUK-134 significantly decreased the number of FPASMC in S phase ($p < 0.05$ versus untreated; Fig. 4) while increasing the number of cells in G_2 phase ($p < 0.05$ versus untreated; Fig. 4). The percentage of cells in G_1 phase was unaffected (Fig. 4).

We then performed quantitative immunocytochemistry to determine if EUK-134 exerts its effect on SMC growth via alterations in proteins that regulate the cell cycle. The results obtained indicated that FPASMC treated with 10 μ*M* EUK-134 for 24 h displayed a significant increase in p21, a protein known to negatively regulate cell growth ($p < 0.05$ versus untreated; Fig. 5). Levels of cyclin A, cyclin D1, and p27 were unchanged by EUK-134 treatment (Fig. 5).

DISCUSSION

Proliferation of vascular SMC contributes to the pathophysiology of both pulmonary and systemic hypertension, atherosclerosis, coronary artery restenosis after angioplasty, and stent placement (18). Increasing evidence suggests that ROS such as superoxide and hydrogen peroxide are important in both proliferation and survival of vascular SMC (5, 16, 23, 24, 26). Accordingly, the production of ROS in the vessel

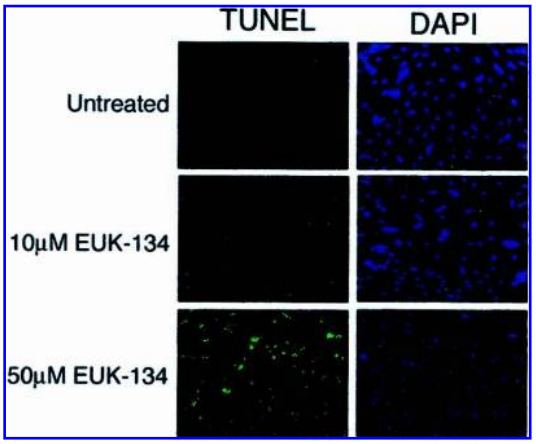

FIG. 2. Low-dose EUK-134 does not induce DNA fragmentation in FPASMC. FPASMC were seeded onto 96-well plates and incubated with 0, 10, or 50 μ*M* EUK-134. After 30 h, TUNEL assays were performed by incubating cells with TdT and reaction mix including fluorescein-12-dUTP for 1 h at 37°C. Cells were then incubated with DAPI (5 μ*M*) for 15 min at room temperature. DAPI is a blue fluorescent nuclear stain, and this step ensured that approximately equal cells were imaged in each slide. As a positive control, 50 μ*M* EUK-134 stimulated FPASMC DNA fragmentation as shown previously (25).

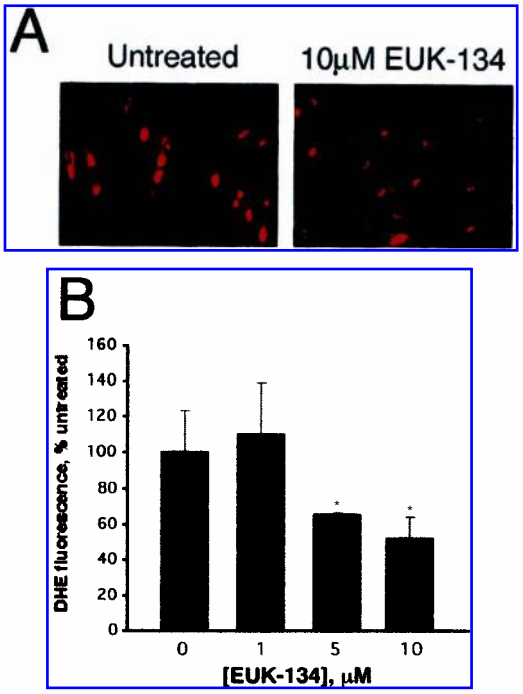

FIG. 3. EUK-134 decreases superoxide levels in FPASMC. Cells were incubated with 0–10 μ*M* EUK-134 for 30 min. DHE at 20 μ*M* was added to the media 15 min before the end of the experiment, and cells were visualized by fluorescent microscopy. (**A**) Representative DHE fluorescent images (captured under identical imaging conditions) of FPASMC treated with 0 and 10 μ*M* EUK-134. (**B**) Dose-dependent decreases in DHE fluorescence in response to treatment with EUK-134. Average fluorescent intensity of each image was quantified using Metamorph imaging software. Values are means ± SD; $n = 4$ samples. $*p < 0.05$ versus untreated cells.

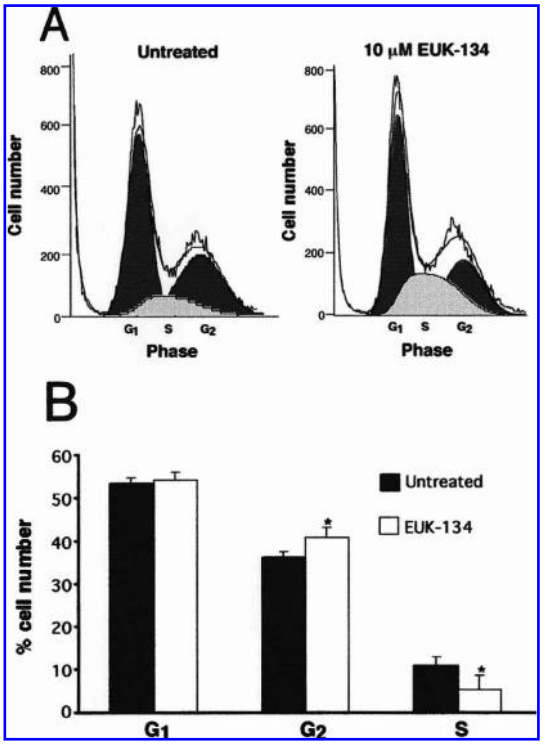

FIG. 4. Changes in FPASMC cell-cycle distribution after exposure to low-dose EUK-134. (**A**) Representative ModFit data from untreated FPASMC and from cells treated with 10 μ*M* EUK-134. (**B**) Changes in FPASMC cell-cycle distribution in response to treatment with 10 μ*M* EUK-134. In untreated samples, 53.2 ± 1.5% of cells were in G_1 phase, 10.7 ± 2.3% were in S phase, and 36.1 ± 1.3% were in G_2 phase. In EUK-134-treated samples, 54.2 ± 1.6% of cells were in G_1 phase, 5.1 ± 3.4% were in S phase, and 40.6 ± 2.4% were in G_2 phase. Values are means ± SD; $n = 3$ samples. $*p < 0.05$ versus untreated cells.

wall is increased in conditions associated with vascular remodeling, including hypercholesterolemia, hypertension, diabetes, and balloon injury to the coronary arteries (10, 13, 14). Furthermore, we have recently demonstrated an increase in superoxide production in the pulmonary arteries of a lamb model of persistent pulmonary hypertension of the newborn (4). Antioxidants that reduce the levels of superoxide and hydrogen peroxide may therefore be of therapeutic benefit in the treatment of various vascular diseases.

We have previously shown the importance of ROS in the regulation of FPASMC growth. Elevation of superoxide hydrogen peroxide levels stimulated FPASMC proliferation, whereas antioxidants inhibited proliferation and at higher doses induced apoptosis (26). Similarly, we recently showed that EUK-134, a superoxide dismutase/catalase mimetic, induced apoptosis at concentrations of 25 μ*M* and above (25). In contrast, in the present study, we found that 5 μ*M* EUK-134 partially abolished, whereas 10 μ*M* EUK-134 completely abolished, serum-induced FPASMC proliferation without reducing the initial number of cells seeded or inducing apoptosis. Overall, these data suggest that the oxidative state of the cell determines FPASMC proliferation and viability. High levels of ROS stimulate a

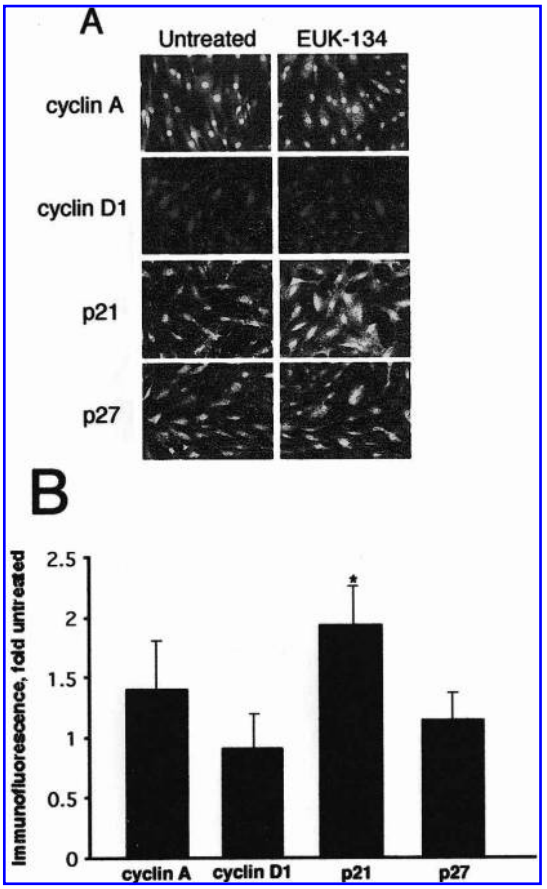

FIG. 5. Immunocytochemistry to detect changes in cell-cycle regulatory proteins after exposure to low dose EUK-134. (**A**) Representative fluorescent images (captured under identical imaging conditions) depicting protein levels and subcellular distribution of cyclin A, cyclin D1, p21, and p27. Cyclin A is required for G_1-to-S phase transition, and decreases in protein levels are associated with growth arrest in G_1 phase. Cyclin D1 regulates the phosphorylation of Rb. p21 and p27 are inhibitors that interfere with cyclin A-mediated cdk activity. Increases in these proteins are associated with growth arrest in G_1 phase. Increases in p21 have also been detected in cells arrested in G_2. (**B**) Average nuclear fluorescent intensity of each image in A was quantified using Metamorph imaging software. Values are means ± SD; $n = 3$ cell samples; $^*p < 0.05$ versus untreated cells.

proliferative pathway, whereas decreases in ROS give a corresponding decrease in FPASMC proliferation until growth arrest occurs. When ROS levels fall below a certain threshold, an apoptotic cascade is triggered that involves loss of mitochondrial membrane potential, caspase-9 and caspase-3 activation, and DNA fragmentation (25). Our combined DHE data suggest that decreases in cellular superoxide levels attenuate serum-induced proliferation. Further, our data indicate that proliferation of FPASMC can be attenuated by a 30% drop in superoxide levels, whereas complete growth arrest occurs when levels drop to ~50% of that of untreated cells. Apoptotic cells then become evident when superoxide levels fall by 80%. Conversely, the difference in H_2DCF-DA fluorescence between growth-attenuated and apoptotic FPASMC is less dramatic. This suggests that superoxide is a major regulator of FPASMC growth and viability, or that more subtle decreases in hydrogen peroxide can stimulate apoptosis. However, titration of ROS with antioxidants such as EUK-134 could potentially be used to specifically modulate FPASMC growth. Thus, in patients with excessively muscularized arteries, high doses of EUK-134 could be used to stimulate apoptosis, thereby decreasing the number of SMC and potentially reversing the vascular remodeling. In less severe cases, administration of lower doses of EUK-134 to inhibit SMC proliferation without inducing cell death may be more desirable.

Cell-cycle progression is mediated by cyclin-dependent kinases (cdk) and their regulatory subunits, the cyclins (21). Cyclin A expression late in G_1 is important for G_1-to-S phase progression, because cyclin A inhibition prevents entry into S phase (15). Members of the cyclin D family regulate the phosphorylation of retinoblastoma protein (Rb), an event essential for cell-cycle progression (7). Cdk inhibitors also regulate cdk activity; p21 and p27 are cdk inhibitors that interfere with cyclin A-mediated cdk activation (22). Furthermore, p21 also blocks the hyperphosphorylation of Rb (11). Once Rb becomes hyperphosphorylated, cell replication no longer requires additional external stimuli. Our flow cytometry analysis identified an increase in the number of FPASMC in G_2 phase after a 24-h exposure to 10 μM EUK-134. This was associated with an increase in p21 protein levels as detected by immunocytochemistry. However, elevated p21 did not affect the number of cells in G_1 phase. Furthermore, EUK-134 treatment did not change the levels of cyclin A, cyclin D1, or p27, other proteins regulating G_1-to-S progression. Overall, our data suggest that EUK-134 attenuates serum-induced FPASMC proliferation via p21-mediated growth arrest in G_2 phase. In support of our conclusions, a recent study found that hyperoxia induced p21 expression in cardiac fibroblasts with an associated growth arrest in G_2, but not in G_1 (19). However, further experiments will be required to identify additional components of this inhibitory pathway.

In a recent study, we found that the nitric oxide (NO) donor spermine NONOate attenuated FPASMC proliferation and at higher doses induced apoptosis (27). NO reacts rapidly with superoxide to form peroxynitrite, and the titration of superoxide may account for the inhibitory effects of NO on FPASMC growth and viability. However, unlike EUK-134 treatment, NO induced FPASMC growth arrest in G_1/S phase associated with a decrease in cyclin A and increased nuclear localization of p21 and p27 (27). This suggests that SMC growth may be regulated via different pathways, depending on the biochemistry of the agent used. The catalase activity of EUK-134 may stimulate antiproliferative pathways that are not triggered by superoxide removal alone. Alternatively, NO-mediated nitrosylation and/or peroxynitrite-mediated nitration of cell-cycle regulatory proteins may account for our observed differences. Interestingly, EUK-134 reduced protein nitration in a mouse model of amyotrophic lateral sclerosis (12) and in kainate-induced neurotoxicity (17). More recently, EUK-134 was shown to react directly with NO and peroxynitrite via oxidant-dependent processes (20). Thus, EUK-134 and NO appear to bring about FPASMC growth arrest and apoptosis via distinctly different mechanisms. However, further characterization of the mecha-

nisms involved may lead to a combined treatment strategy for pulmonary vascular remodeling that proves more effective than the use of single antioxidant molecules alone.

ACKNOWLEDGMENTS

This research was supported in part by grants HD398110 (to S.M.B.), HL67841 (to S.M.B.), HL072123 (to S.M.B.), and HL070061 (to S.M.B.) from the National Institutes of Health, FY00–98 from the March of Dimes (to S.M.B.), and 0330292N from the American Heart Association National Office (to S.W.).

ABBREVIATIONS

cdk, cyclin-dependent kinase; DAPI, 4′,6-diamidino-2-phenylindole; DHE, dihydroethidium; DMEM, Dulbecco's modified Eagle's medium; FPASMC, fetal pulmonary arterial smooth muscle cells; H_2DCF-DA, dichlorodihydrofluorescein diacetate; NO, nitric oxide; PBS, phosphate-buffered saline; Rb, retinoblastoma protein; ROS, reactive oxygen species; SMC, smooth muscle cells; TdT, terminal deoxynucleotidyltransferase; TUNEL, terminal deoxynucleotidyltransferased UTP nick end-labeling.

REFERENCES

1. Anderson I, Adinolfi C, Doctrow SR, Huffman K, Joy KA, Malfroy B, Soden P, Rupniak HT, and Barnes JC. Oxidative signalling and inflammatory pathways in Alzheimer's disease. *Biochem Soc Symp* 141–149, 2001.
2. Baker K, Marcus CB, Huffman K, Kruk H, Malfroy B, and Doctrow SR. Synthetic combined superoxide dismutase/catalase mimetics are protective as a delayed treatment in a rat stroke model: a key role for reactive oxygen species in ischemic brain injury. *J Pharmacol Exp Ther* 284: 215–221, 1998.
3. Baudry M, Etienne S, Bruce A, Palucki M, Jacobsen E, and Malfroy B. Salen-manganese complexes are superoxide dismutase-mimics. *Biochem Biophys Res Commun* 192: 964–968, 1993.
4. Brennan LA, Steinhorn RH, Wedgwood S, Mata-Greenwood E, Roark EA, Russell JA, and Black SM. Increased superoxide generation is associated with pulmonary hypertension in fetal lambs: a role for NADPH oxidase. *Circ Res* 92: 683–691, 2003.
5. Brown MR, Miller FJ, Li WG, Ellingson AN, Mozena JD, Chatterjee PK, Engelhardt JF, Zwacka RM, Oberley LW, Fang X, Spector AA, and Weintraub NL. Overexpression of human catalase inhibits proliferation and promotes apoptosis in vascular smooth muscle cells. *Circ Res* 85: 524–533, 1999.
6. Cory AH, Owen TC, Barltrop JA, and Cory JG. Use of an aqueous soluble tetrazolium/formazan assay for cell growth assays in culture. *Cancer Commun* 3: 207–212, 1991.
7. Dowdy SF, Hinds PW, Louie K, Reed SI, Arnold A, and Weinberg RA. Physical interaction of the retinoblastoma protein with human D cyclins. *Cell* 73: 499–511, 1993.
8. Gonzalez PK, Zhuang J, Doctrow SR, Malfroy B, Benson PF, Menconi MJ, and Fink MP. EUK-8, a synthetic superoxide dismutase and catalase mimetic, ameliorates acute lung injury in endotoxemic swine. *J Pharmacol Exp Ther* 275: 798–806, 1995.
9. Griendling KK, Minieri CA, Ollerenshaw JD, and Alexander RW. Angiotensin II stimulates NADH and NADPH oxidase activity in cultured vascular smooth muscle cells. *Circ Res* 74: 1141–1148, 1994.
10. Grunfeld S, Hamilton CA, Mesaros S, McClain SW, Dominiczak AF, Bohr DF, and Malinski T. Role of superoxide in the depressed nitric oxide production by the endothelium of genetically hypertensive rats. *Hypertension* 26: 854–857, 1995.
11. Harper JW, Adami GR, Wei N, Keyomarsi K, and Elledge SJ. The p21 Cdk-interacting protein Cip1 is a potent inhibitor of G1 cyclin-dependent kinases. *Cell* 75: 805–816, 1993.
12. Jung C, Rong Y, Doctrow SR, Baudry M, Malfroy B, and Xu Z. Synthetic superoxide dismutase/catalase mimetics reduce oxidative stress and prolong survival in a mouse amyotrophic lateral sclerosis model. *Neurosci Lett* 304: 157–160, 2001.
13. Langenstroer P and Pieper GM. Regulation of spontaneous EDRF release in diabetic rat aorta by oxygen free radicals. *Am J Physiol* 263: H257–H265, 1992.
14. Ohara Y, Peterson TE, and Harrison DG. Hypercholesterolemia increases endothelial superoxide anion production. *J Clin Invest* 91: 2546–2551, 1993.
15. Pagano M, Pepperkok R, Verde F, Ansorge W, and Draetta G. Cyclin A is required at two points in the human cell cycle. *EMBO J* 11: 961–971, 1992.
16. Rao GN and Berk BC. Active oxygen species stimulate vascular smooth muscle cell growth and proto-oncogene expression. *Circ Res* 18: 775–794, 1992.
17. Rong Y, Doctrow SR, Tocco G, and Baudry M. EUK-134, a synthetic superoxide dismutase and catalase mimetic, prevents oxidative stress and attenuates kainate-induced neuropathology. *Proc Natl Acad Sci U S A* 96: 9897–9902, 1999.
18. Ross R. A pathogenesis of atherosclerosis: a perspective for the 1990s. *Nature* 362: 801–809, 1993.
19. Roy S, Khanna S, Bickerstaff AA, Subramanian SV, Atalay M, Bierl M, Pendyala S, Levy D, Sharma N, Venojarvi M, Strauch A, Orosz CG, and Sen CK. Oxygen sensing by primary cardiac fibroblasts: a key role of p21(Waf1/Cip1/Sdi1). *Circ Res* 92: 264–271, 2003.
20. Sharpe MA, Ollosson R, Stewart VC, and Clark JB. Oxidation of nitric oxide by oxomanganese-salen complexes: a new mechanism for cellular protection by superoxide dismutase/catalase mimetics. *Biochem J* 366: 97–107, 2002.
21. Sherr CJ. Cancer cell cycles. *Science* 274: 1672–1677, 1996.
22. Sherr CJ and Roberts JM. Inhibitors of mammalian G1 cyclin-dependent kinases. *Genes Dev* 9: 1149–1163, 1995.
23. Sundaresan M, Yu ZX, Ferrans VJ, Irani K, and Finkel T. Requirement for generation of H_2O_2 for platelet-derived growth factor signal transduction. *Science* 270: 296–299, 1995.
24. Tsai JC, Jain M, Hsieh CM, Lee WS, Yoshizumi M, Patterson C, Perralla MA, Cook C, Wang H, Haber E, Schlegal R, and Lee ME. Induction of apoptosis by pyrrolidinedithio-

carbamate and *N*-acetylcysteine in vascular smooth muscle cells. *J Biol Chem* 271: 3667–3670, 1996.
25. Wedgwood S and Black SM. Induction of apoptosis in fetal pulmonary arterial smooth muscle cells by a combined superoxide dismutase/catalase mimetic. *Am J Physiol Lung Cell Mol Physiol* 285: L305–L312, 2003.
26. Wedgwood S, Dettman RW, and Black SM. ET-1 stimulates pulmonary arterial smooth muscle cell proliferation via induction of reactive oxygen species. *Am J Physiol Lung Cell Mol Physiol* 281: L1058–L1067, 2001.
27. Wedgwood S, Brennan LA, Lu J, Jilling T, and Black SM. Biphasic effects of nitric oxide on fetal pulmonary arterial smooth muscle cell growth. *Pediatr Res* 51: 390A, 2002.
28. Wedgwood S, Mitchell CJ, Fineman JR, and Black SM. Developmental differences in the shear stress-induced expression of endothelial NO synthase: changing role of AP-1. *Am J Physiol Lung Cell Mol Physiol* 284: L650–L662, 2003.

Address reprint requests to:
Stephen M. Black, Ph.D.
Director of Vascular Biology
International Heart Institute of Montana
St. Patrick Hospital
500 W. Broadway
Missoula, MT 59802

E-mail: smblack@selway.umt.edu

Received for publication June 19, 2003; accepted September 30, 2003.

This article has been cited by:

1. Hyo Jung Kim, Byung-Yoon Cha, Bongkeun Choi, Ji Sun Lim, Je-Tae Woo, Jong-Sang Kim. 2011. Glyceollins inhibit platelet-derived growth factor-mediated human arterial smooth muscle cell proliferation and migration. *British Journal of Nutrition* 1-12. [CrossRef]
2. Yuansheng Gao, J Usha RajHypoxic Pulmonary Hypertension of the Newborn . [CrossRef]
3. Irina I. Rudneva, Ekaterina N. Skuratovskaya, Natalya S. Kuzminova, Tatyana B. Kovyrshina. 2010. Age composition and antioxidant enzyme activities in blood of Black Sea teleosts. *Comparative Biochemistry and Physiology Part C: Toxicology & Pharmacology* **151**:2, 229-239. [CrossRef]
4. Shing-Jong Lin, Song-Kun Shyue, Meng-Chun Shih, Ting-Hui Chu, Yung-Hsiang Chen, Hung-Hai Ku, Jaw-Wen Chen, Ka-Bik Tam, Yuh-Lien Chen. 2007. Superoxide dismutase and catalase inhibit oxidized low-density lipoprotein-induced human aortic smooth muscle cell proliferation: Role of cell-cycle regulation, mitogen-activated protein kinases, and transcription factors. *Atherosclerosis* **190**:1, 124-134. [CrossRef]
5. Yuichiro J. Suzuki , Hiroko Nagase , Kai Nie , Ah-Mee Park . 2005. Redox Control of Growth Factor Signaling: Recent Advances in Cardiovascular Medicine. *Antioxidants & Redox Signaling* **7**:5-6, 829-834. [Abstract] [PDF] [PDF Plus]